High-Resolution Electron Energy-Loss Studies of Hydrocarbon Formation from Methane Decomposition on Ru(0001) and Ru(11$\bar{2}$0) Catalysts

Ming-Cheng Wu and D. Wayne Goodman*

Contribution from the Department of Chemistry, Texas A&M University, College Station, Texas 77843-3255

Received June 1, 1993®

Abstract: The reaction of methane with single-crystal ruthenium catalysts has been studied utilizing an elevated-pressure microreactor (contiguous to a surface analysis system), high-resolution electron energy-loss spectroscopy (HREELS), and temperature-programmed desorption (TPD). Methane is found to dissociate on Ru(0001) and Ru(11$\bar{2}$0) surfaces to form various hydrocarbon intermediates. On the Ru(11$\bar{2}$0) surface, three distinct forms of surface hydrocarbon species are identified: methylidyne (CH), vinylidene (CCH_2) and ethylidyne (CCH_3). On the Ru(0001) surface only the methylidyne and vinylidene species were observed. At reaction temperatures exceeding 700 K, no loss features associated with surface hydrocarbon species are found. HREELS measurements and CO titration experiments indicate the presence of a surface graphitic phase at temperatures >700 K. A comparison is also made between the surface carbon species found in the present study and the carbon types found on supported catalysts.

1. Introduction

The chemical conversion of methane to higher hydrocarbons is an important area of current catalytic research. Methane, in comparison with other classes of organic molecules, is thermodynamically more stable and extremely unreactive at surfaces. This feature makes the conversion of methane particularly challenging. A current strategy for methane conversion utilizes an indirect route in which methane is first reacted with water to form carbon monoxide and hydrogen over a supported Ni catalyst. In the second step, the synthesis gas is converted to higher hydrocarbons via either Fischer–Tropsch or methanol synthesis.[1,2] An intriguing approach for direct carbon–carbon coupling from methane is the oxidative coupling of methane to ethane/ethylene over metal oxide catalysts.[3-7] This reaction proceeds at temperatures between 850 and 1200 K with C_2 hydrocarbon yields of approximately 20%.[4]

The present work stems from recent investigations by van Santen and co-workers,[10] who have used an alternate route to higher hydrocarbons from methane. This approach involves the dissociation of methane to hydrocarbonaceous residues over a transition-metal catalyst at temperatures between 350 and 850 K. The surface carbon intermediates then are polymerized and rehydrogenated to C_2 hydrocarbons at ~370 K.[8,9] The maximum C_2 yield achieved using this approach from a supported ruthenium catalyst is 13%.[8,9]

Several theoretical studies[10-13] have been carried out to elucidate the reaction mechanisms for carbon–carbon bond formation between surface carbon fragments. The initial efforts have been focused on the recombination of highly hydrogenated CH_x species because these fragments are predicted to be highly mobile on the surface.[11] Accordingly, nearly all combinations of CH_x fragments have been tried. Zheng and co-workers,[12] for example, have studied the coupling between two surface methyl groups on a Co(0001) surface but found no reaction path for coupling with an acceptable low activation energy. Recently, van Santen's group has carried out an extensive theoretical study for the recombination of surface CH_x species on several transition-metal surfaces.[10,11] Using semiempirical quantum-chemical calculations, these authors found that highly hydrogenated surface carbonaceous fragments all have high activation energies for recombination. This is due to repulsion between the hydrogen atoms of these hydrogen-rich carbon species. The lowest activation energy was found for the coupling between a threefold bonded carbon atom and a methylidene (CH_2) species to form a vinylidene (CCH_2) intermediate.[10,11]

In contrast to the case of the above theoretical investigations, little experimental effort has been made to detect directly these surface intermediates using single crystals and modern surface science techniques. It has been shown that the detection, by Auger electron spectroscopy (AES)[14] and photoelectron spectroscopy,[15,16] of fractional monolayers of carbon on ruthenium is difficult because of the interference of the substrate signals. Using AES, Goodman and White[14] found an AES feature, assigned to carbidic carbon, that was separable from the Ru features. In the present study, high-resolution electron energy-loss spectroscopy (HREELS) has been used to identify surface hydrocarbonaceous intermediates formed from methane decomposition on ruthenium single-crystal surfaces.

Among the various surface spectroscopic techniques used to characterize adsorbate properties, HREELS is a powerful tool for identifying rather complex molecular adsorbates by their characteristic vibrational frequencies (fingerprints). To date, a large body of HREELS data of hydrocarbon species on transition-metal surfaces is available in the literature. Of particular relevance to the present study are HREELS studies of the

* Abstract published in *Advance ACS Abstracts,* February 1, 1994.

(1) Rostrup-Nielsen, J. R. Catalysis: Science and Technology; Anderson, J. R., Boudart, M., Eds.; Springer-Verlag: Heidelberg, Germany, 1984.
(2) Anderson, J. R. *Appl. Catal.* **1989**, *47*, 177–196.
(3) Hutchings, G. J.; Scurrel, M. S.; Woodhouse, J. R. *Chem. Soc. Rev.* **1989**, *18*, 251–283.
(4) Lunsford, J. H. *Catal. Today* **1990**, *6*, 235–259.
(5) Ito, T.; Lunsford, J. H. *Nature (London)* **1985**, *314*, 721–722.
(6) Driscoll, D. J.; Martir, W; Wang, J.-X.; Lunsford, J. H. *J. Am. Chem. Soc.* **1985**, *107*, 58–63.
(7) Ito, T.; Wang, J.-X.; Lin, C.-H.; Lunsford, J. H. *J. Am. Chem. Soc.* **1985**, *107*, 5062–5068.
(8) Koerts, T.; van Santen, R. A. *J. Molec. Catal.* **1991**, *70*, 119–127.
(9) Koerts, T.; van Santen, R. A. *J. Chem. Soc., Chem. Commun.* **1991**, 1281–1283.
(10) Koerts, T.; Deelen, M. J. A. G.; van Santen, R. A. *J. Catal.* **1992**, *138*, 101–114.
(11) Koster, A. De.; van Santen, R. A. *J. Catal.* **1991**, *127*, 141–166.
(12) Zheng, C; Apeloig, Y.; Hoffman, R. *J. Am. Chem. Soc.* **1988**, *110*, 749–774.
(13) Feibelman, P. J. *Phys. Rev. B* **1982**, *26*, 5347–5355.
(14) Goodman, D. W.; White, J. M. *Surf. Sci.* **1979**, *90*, 201–203.
(15) Hrbek, J. *J. Vac. Sci. Technol.* **1986**, *4*, 86–89.
(16) Himpsel, F. J.; Christmann, K.; Heimann, P; Eastman, D. E.; Feibelman, P. J. *Surf. Sci.* **1982**, *115*, L159–164.

0002-7863/94/1516-1364$04.50/0

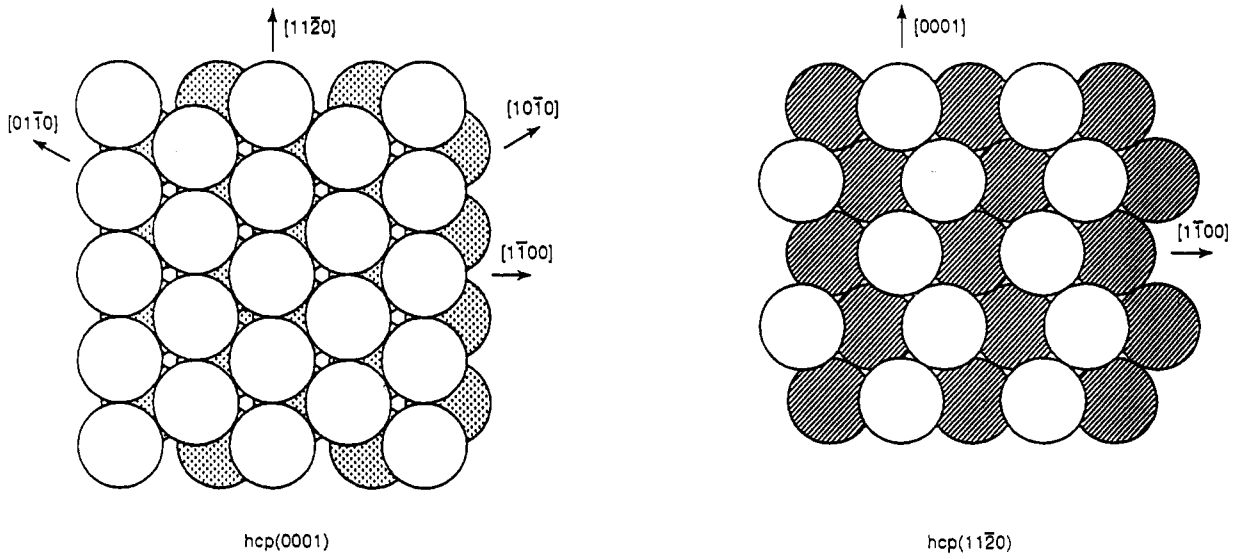

Figure 1. Ru(0001) and Ru(11$\bar{2}$0) surface structures.

chemisorption and decomposition of acetylene and ethylene on single-crystal transition metal surfaces.[17-35] These studies provide extremely useful information regarding various hydrocarbon species and their characteristic vibrational frequencies. Such knowledge is critical to the assignment of the loss features observed in the present study.

A general trend revealed in these HREELS studies[17-35] is that both acetylene and ethylene adsorb associatively at temperatures near 100 K and decompose upon heating into various hydrocarbon intermediates. HREELS spectra of ethylene decomposition, for example, showed that upon heating, either ethylidyne (CCH_3) (Ru(0001),[17-20] Rh(111),[21,22] Pd(111),[23] and Pt(111)[24]) or acetylene and hydrogen (Ni(111),[25,26] Fe(110),[29] and W(100)[30]) are formed. In some cases, the presence of acetylide (CCH) was also reported (Ru(0001),[17,18] Pd(100),[31] and Ni(110)[32]). The decomposition products of acetylene were found to be primarily methylidyne (CH), which further decomposes into carbon atoms at higher temperatures.[28-32] One exception to this trend appears to be a stepped Ni[5(111)x(1$\bar{1}$0)] surface, where, even at 150 K, acetylene dehydrogenates to a metastable surface species of C_2.[26] In the present study, we exploit these early successes to identify various intermediates from methane decomposition on Ru surfaces.

2. Experimental Details

2.1. Apparatus. The studies were carried out in a combined elevated-pressure reactor/ultrahigh vacuum (UHV) system equipped with HREELS, Auger electron spectroscopy (AES), low-energy electron diffraction (LEED), and temperature programmed desorption (TPD). The details of this UHV system have been described elsewhere.[36] After completion of surface cleaning in the spectroscopic chamber, the single-crystal Ru catalyst could be transferred in situ into the reaction chamber through a double-stage differentially pumped Teflon sliding seal.

Schematic drawings of the Ru(0001) and Ru(11$\bar{2}$0) surfaces are shown in Figure 1. The single-crystal samples could be resistively heated to 1500 K and cooled to 90 K. The UHV system also has capabilities for electron-beam heating of the sample to temperatures above 1500 K. Sample temperatures were monitored with W-5%Re/W-26%Re thermocouple wires spot-welded to the edge of the rear surface.

2.2. Crystal Cleaning. The crystal-cleaning procedure consisted of oxidation in 1×10^{-7} Torr of oxygen at 900–1300 K for 5–10 min and a flash to 1700–1800 K. After several cycles of the above procedure, impurities (mainly carbon and oxygen) were below the detection limit of AES. Low-energy electron-diffraction studies showed a sharp (1×1) LEED pattern of these crystal faces. An HREELS spectrum, however, usually exhibited a weak loss feature at 445 cm^{-1} after the above cleaning procedure. Heating the crystals in a few torr of hydrogen or methane eliminated this peak completely. We attribute the 445 cm^{-1} loss peak to an oxygen species in the near-surface region. The previous work of Surney et al.[37] has demonstrated that appreciable oxygen diffusion into the Ru lattice can occur during annealing in the 1150–1700 K temperature range.

2.3. Gas Handling and Purity. Methane gas was purchased from Matheson at a nominal purity of 99.996%. Of key concern in our experiments was the purity of the gases. We used the following procedure for gas purification: (1) storage in a zeolite-filled trap which was immersed in a liquid-nitrogen Dewar; (2) release of CH_4 by warming up this trap until the desired CH_4 pressure was obtained in the manifold; (3) subsequent storage in a glass bulb whose inner wall was coated with freshly deposited titanium before admission into the reaction chamber. The above procedure has been extremely effective in removing impurity gases from methane.[38,39] Our HREELS measurements showed that, after reaction, impurities from the purified CH_4 gas were below the detection limit of the instrument.

2.4. Reaction Methods. The following procedure was used in carrying out a reaction: (1) Purified methane gas was introduced into the reactor with the clean crystal at $T < 330$ K; (2) the crystal temperature was

(17) Parmeter, J. E.; Hills, M. M.; Weinberg, W. H. *J. Am. Chem. Soc.* **1986**, *108*, 3563–3569.
(18) Hills, M. M.; Parmeter, J. E.; Mullins, C. B.; Weinberg, W. H. *J. Am. Chem. Soc.* **1986**, *108*, 3554–3562.
(19) Henderson, M. A.; Mitchell, G. E.; White, J. M. *Surf. Sci.* **1988**, *203*, 378–394.
(20) Jakob, P.; Cassuto, A.; Menzel, D. *Surf. Sci.* **1987**, *187*, 407–433.
(21) Dubois, L. H.; Castner, D. G.; Somorjai, G. A. *J. Chem. Phys.* **1980**, *72*, 5234–5240.
(22) Koel, B. E.; Bent, B. E.; Somorjai, G. A. *Surf. Sci.* **1984**, *146*, 211–228.
(23) Kesmodel, L. L.; Gates, J. A. *Surf. Sci.* **1981**, *111*, L747–L754.
(24) Steininger, H.; Ibach, H.; Lehwald, S. *Surf. Sci.* **1982**, *117*, 685–698.
(25) Bertolini, J. C.; Rousseau, J. *Surf. Sci.* **1979**, *83*, 531–544.
(26) Lehwald, S.; Ibach, H. *Surf. Sci.* **1979**, *89*, 425–445.
(27) Lee, M. B.; Yang, Q. Y.; Ceyer, S. T. *J. Chem. Phys.* **1987**, *87*, 2724–2741.
(28) Demuth, J. E.; Ibach, H. *Surf. Sci.* **1978**, *78*, L238–L244.
(29) Erley, W.; Baro, A. M.; Ibach, H. *Surf. Sci.* **1982**, *120*, 273–290.
(30) Hamilton, J. C.; Swanson, N.; Waclawski, B. J.; Celotta, R. J. *J. Chem. Phys.* **1981**, *74*, 4156–4163.
(31) Kesmodel, L. L. *J. Vac. Sci. Technol. A* **1984**, *2*, 1083–1084.
(32) Stroscio, J. A.; Bare, S. R.; Ho, W. *Surf. Sci.* **1984**, *148*, 499–525.
(33) Chen, J. G.; Beebe, T. P., Jr.; Crowell, J. E.; Yates, J. T., Jr. *J. Am. Chem. Soc.* **1987**, *109*, 1726–1729.
(34) Bandy, B. J.; Chesters, M. A.; Pemble, M. E.; McDougall, G. S.; Sheppard, N. *Surf. Sci.* **1984**, *139*, 87–97.
(35) Hengrasmee, S.; Peel, J. B. *Surf. Sci.* **1987**, *184*, 434–448.
(36) Wu, M.-C.; Estrada, C. A.; Corneille, J. S.; Goodman, D. W. *J. Chem. Phys.* **1992**, *96*, 3892–3900.
(37) Surney, L.; Rangelov, G.; Bliznakov, G. *Surf. Sci.* **1985**, *159*, 299–310.
(38) Beebe, T. P., Jr.; Goodman, D. W.; Kay, B. D.; Yates, J. T., Jr. *J. Chem. Phys.* **1987**, *87*, 2305–2315.
(39) Campbell, R. A.; Szanyi, J.; Lenz, P.; Goodman, D. W. *Catal. Lett.* **1993**, *17*, 39–46.

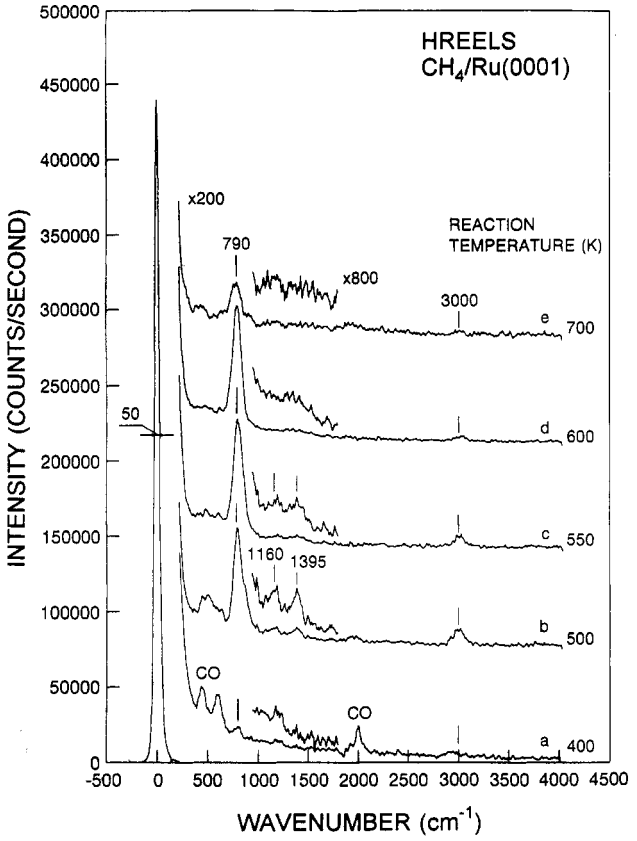

Figure 2. HREELS spectra acquired following methane decomposition on Ru(0001) as a function of the reaction temperature (sample temperature, T). The reaction was carried out with 5 Torr of methane for 120 s. The spectra were collected at $E_p \simeq 4.1$ eV and at the specularly reflected beam direction.

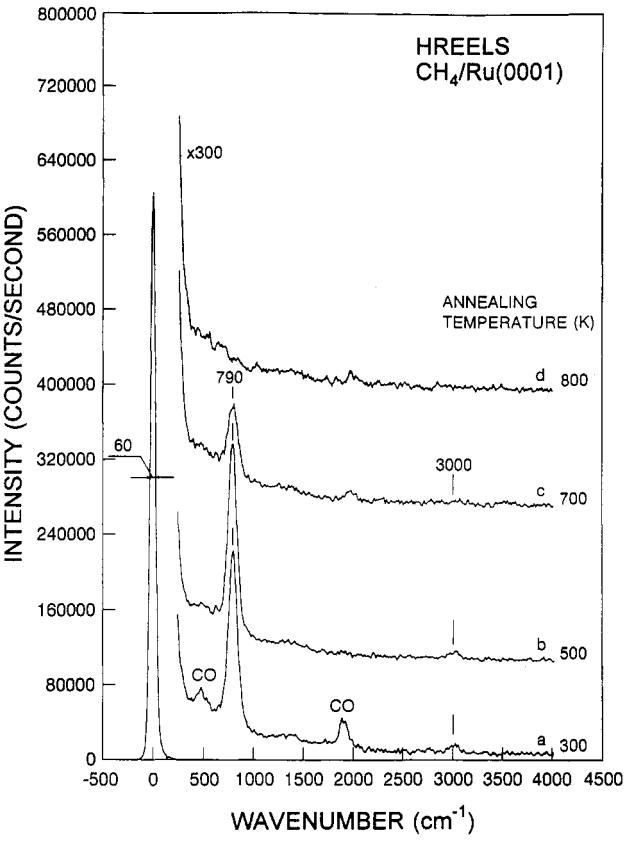

Figure 3. Thermal stability of methylidyne under UHV conditions. The reaction was carried out with 5 Torr of methane at 600 K for 120 s. Note that the upper curve, acquired following an anneal to 800 K, exhibits a spectrum nearly indistinguishable from that of the clean surface; however, both Auger measurements and CO titration indicate the presence of surface graphitic carbon species. The spectra were collected at $E_p \simeq 4.1$ eV and at the specularly reflected beam direction.

quickly raised to a reaction temperature where it was held by using a temperature controller for the length of that particular reaction (typically 120 s); (3) heating was turned off simultaneously while exhausting the gas; (4) the crystal was transferred to the EELS position of the surface analytical chamber. The pressure, P, in the surface analytical chamber was increased during step 4 but was decreased to $P \simeq 5 \times 10^{-10}$ Torr within a minute. Subsequent EELS measurements were carried out at room temperature and at $P < 2 \times 10^{-10}$ Torr.

2.5. HREELS Data Acquisition. The HREELS spectra were acquired using an electron beam with a primary energy of $E_p \simeq 2$–4 eV and an incident angle of 60° from the surface normal. The other parameters used in obtaining the EELS spectra presented here were the following: spectral resolution (full width at half maximum of the elastically reflected electron beam), 50–60 cm^{-1}; typical count rate in the elastic peak of the clean surface, 500 000 Hz. The reaction of methane with the ruthenium crystals under the present experimental conditions does not affect the count rate in the elastic peak nor the spectral resolution.

3. Results

3.1. Reaction of Methane with Ru(0001). The reaction of CH_4 with a Ru(0001) surface has been carried out in the reaction chamber with 5 Torr of methane for 120 s and subsequently examined in the surface analytical chamber using HREELS. Displayed in Figure 2 are HREELS spectra acquired following methane decomposition on Ru(0001) as a function of the reaction temperature (sample temperature, T). The HREELS data presented here were collected after momentarily heating the sample to 500 K in the UHV chamber to remove a small amount of adsorbed CO. Exposing the surface to methane gives rise to several distinct loss features in the 200–4000-cm^{-1} frequency range of the HREELS spectra. Two sets of loss features can be easily recognized from Figure 2. A dominant loss peak at 790 cm^{-1} and a weak feature at 3000 cm^{-1} are observed in the 400–700 K temperature range, while two weaker loss peaks at 1160 and 1395 cm^{-1} are evident only at temperatures between 500 and 550 K in the HREELS spectra. These two sets of loss peaks apparently arise from two different surface intermediates. In the following sections, the losses at 790 and 3000 cm^{-1} are attributed to the CH bending mode (δ(CH)) and the CH stretching mode (ν(CH)), respectively, of a methylidyne species (CH). Likewise, the two weaker loss features at 1160 and 1395 cm^{-1} arise from the carbon–carbon stretch (ν(C=C)) and the CH_2 scissors, respectively, of a vinylidene species (CCH_2). Note that the loss features arising from the methylidyne species at $T = 400$ K have become extremely weak, clearly indicating that methane dissociation on Ru(0001) is an activated process. The details of the kinetic measurements of methane activation on the Ru crystals will be presented elsewhere.[40] Two weak loss features at 475 and 2000 cm^{-1}, which arise from CO adsorbates, are noticeable at this low reaction temperature, as seen in spectrum a of Figure 2. One also observes a weak peak at ~600 cm^{-1}, which probably arises from a subsurface oxygen species.

Figure 3 shows the thermal stability of the losses at 790 and 3000 cm^{-1}. The reaction was carried out with 5 Torr of CH_4 at 600 K for 120 s. Spectrum a of Figure 3 was obtained after reaction without annealing in the spectroscopic chamber. The loss features at 475 and 1905 cm^{-1} are observable in this case and are due to excitations of the CO–metal stretch and the C–O stretch, respectively, of adsorbed CO. Since the cross section of the CO vibrational modes is some 20 times higher than those of hydrocarbon vibrations for electron excitation, the level of CO contamination can be estimated from the relative mode intensities of spectrum a to be negligibly low (<1% monolayer). Heating

(40) Lenz-Solomun, P.; Wu, M.-C.; Goodman, D. W. *Catal. Lett.*, in press.

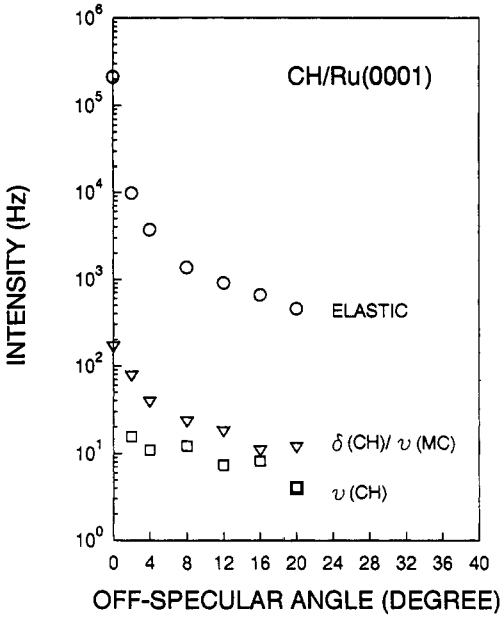

Figure 4. Angle dependence of the loss modes of a CH intermediate. The change of the δ(CH)/ν(MC) mode intensity at 790 cm^{-1} as a function of the off-specular angle was found to parallel the change of the elastic-peak intensity, whereas the 3000-cm^{-1} loss (ν(CH)) remained essentially constant in intensity. The reaction conditions used in obtaining the intensities of these losses were the same as those used in Figure 3.

the sample to 500 K under UHV conditions removes the CO impurities completely, as shown in spectrum b of Figure 3. Since CO contamination is insignificant, further discussions will not address this issue. At annealing temperatures exceeding 700 K, no loss peak is found in the 200–4000-cm^{-1} frequency range except a barely perceptible feature between approximately 1100 and 1500 cm^{-1} which occurs throughout the spectra of Figure 3. In off-specular measurements, this loss feature becomes more intense. In the following section, we will discuss this feature together with CO titration experiments and associate it with surface graphitic carbon. To identify various surface intermediates unambiguously, we have also carried out HREELS measurements at several off-specular directions.

Figure 4, for example, shows intensities of the 790- and 3000-cm^{-1} losses as a function of the off-specular angle of the energy analyzer. The reaction conditions used in obtaining the intensities of these losses were the same as those used in Figure 3. The change of the 790-cm^{-1} loss (δ(CH)) intensity versus the off-specular angle parallels the change of the elastic-peak intensity, whereas the 3000-cm^{-1} loss feature (ν(CH)) remains essentially constant in intensity.

3.2. Reaction of Methane with Ru(11$\bar{2}$0). The reaction of CH_4 with a Ru(11$\bar{2}$0) surface has also been carried out with 5 Torr of methane for 120 s and subsequently examined in the surface analytical chamber using HREELS. Figure 5 shows HREELS spectra acquired of a Ru(11$\bar{2}$0) surface following reaction with methane as a function of the reaction temperature (sample temperature, T). Similar to the case of decomposition of CH_4 on Ru(0001), two sets of loss features are easily recognizable at $T \geq 500$K. These correspond to two different surface intermediates: methylidyne (CH) and vinylidene (CCH_2). Two loss peaks observed at 830 and 3010 cm^{-1} arise from one type of surface species (methylidyne), and losses at ~345, 1165, 1410, 1620, and 2985 cm^{-1} are due to the other (vinylidene). The detailed assignment of these loss features and identification of the corresponding surface species will be given in the following sections. In contrast to the case of methane decomposition on Ru(0001), methane reacts with Ru(11$\bar{2}$0) to form various intermediates even at $T \leq 400$ K, as shown in spectrum a of Figure 5.

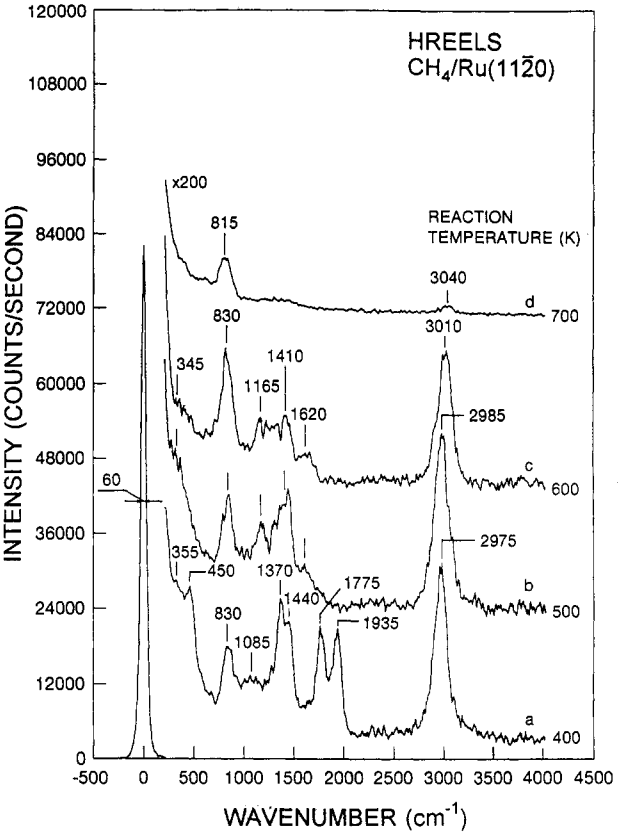

Figure 5. HREELS spectra acquired following methane decomposition on Ru(11$\bar{2}$0) as a function of the reaction temperature (sample temperature, T). The reaction was carried out with 5 Torr of methane for 120 s. The spectra were collected at $E_p \simeq 2.2$ eV and at the specularly reflected beam direction.

Besides the loss features arising from a methylidyne species, a new set of loss peaks is observed at ~355, 1085, 1370, 1440, and 2975 cm^{-1}, as shown in spectrum a of Figure 5. These features apparently arise from a new surface species which differs from CH and CCH_2. The additional losses at 450, 1775, and 1935 cm^{-1} are due to CO adsorbates. Considering the high cross section of CO vibrational modes, the coverage of the CO impurities is extremely low.

Figures 6 and 7 show a series of HREELS spectra acquired after reaction with methane at two representative reaction temperatures of 330 and 500 K, respectively, versus the UHV annealing temperature. These reactions were carried out with 5 Torr of methane for 120 s. As shown in Figure 6, an anneal to 500 K results in an increase in intensity of the 830-cm^{-1} loss, disappearance of the loss features associated with the new species, and the presence of loss features at 1155, 1380, and 1650 cm^{-1} associated with the surface CCH_2 species. At annealing temperatures exceeding 600 K, only the loss peaks arising from surface CH species are visible. Disappearance of these loss features is complete at temperatures exceeding 700 K. Figure 7 shows a similar evolution of the surface intermediates upon annealing. The loss features of the methylidyne are evident up to 700 K, while those of the vinylidene are observed in a lower temperature range between 500 and 600 K.

4. Discussion

4.1. Spectroscopic Identification of Hydrocarbon Species from Methane Decomposition on Ru Surfaces. To facilitate the assignments of the observed vibrational losses and the corresponding surface species, we have used the following strategy: (1) comparison with results of UHV HREELS studies of various hydrocarbon species on transition metals and those obtained from the corresponding organometallic compounds and (2) specular

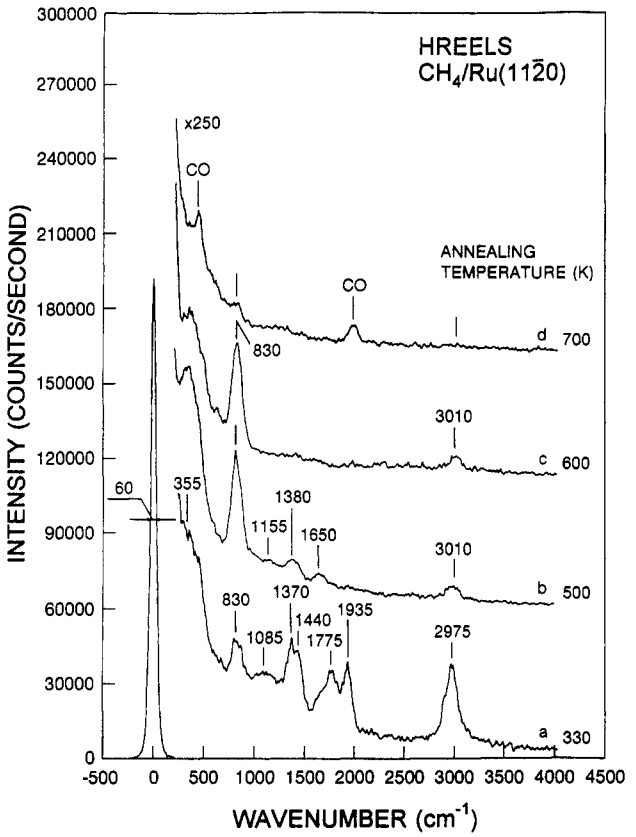

Figure 6. HREELS spectra acquired after methane activation over a Ru(11$\bar{2}$0) surface as a function of the UHV annealing temperature. The reaction of methane with a Ru(11$\bar{2}$0) catalyst was carried out at the reaction temperature of 330 K with 5 Torr CH_4 for 120 s. The spectra were collected at $E_p \simeq 2.2$ eV and at the specularly reflected beam direction.

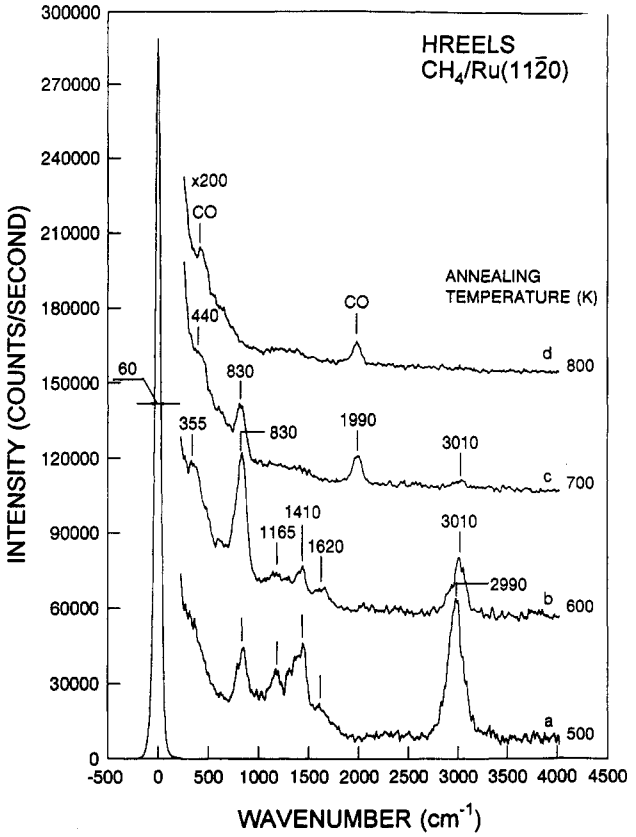

Figure 7. HREELS spectra acquired following methane decomposition on a Ru(11$\bar{2}$0) surface versus the UHV annealing temperature. The reaction of methane with a Ru(11$\bar{2}$0) catalyst was carried out at the reaction temperature of 500 K with 5 Torr CH_4 for 120 s. The spectra were collected at $E_p \simeq 2.2$ eV and at the specularly reflected beam direction.

and off-specular measurements of a vibrational mode which illucidate the excitation mechanism (the dipole versus the impact scattering mechanism) of that vibrational loss. These measurements further aid the assignments of the observed loss features.

We will not consider here an assignment of the observed losses to hydrocarbons higher than C_2 species, since our kinetic studies carried out under identical reaction conditions show that C_3 and higher products are less than 1% of the total yield.[40] These results suggest that hydrocarbon intermediates containing three or more carbon atoms are likely less than 1% of a monolayer. Therefore, the concentration of the C_3 and higher species is very likely below the detection limit of HREELS.

In the preceding section, we have shown that methane decomposition on the Ru surfaces gives rise to separable sets of losses that can be unambiguously attributed to different surface intermediates. The corresponding spectral features are therefore discussed separately.

4.1.1. CH_x Fragments: Methylidyne. One set of losses separable from the remaining losses on both the Ru(0001) and the Ru(11$\bar{2}$0) surfaces is the features near 800 and 3000 cm^{-1}. These losses appear in a wide temperature range and exhibit a distinct loss intensity pattern, i.e. an intense loss at ~800 cm^{-1} and a weak feature at ~3000 cm^{-1}. By analogy to the results obtained from HREELS studies[17,18,20,26-32] and those of organometallic compounds,[41,42] the losses near 800 and 3000 cm^{-1} can be attributed to the CH bending mode (δ(CH)) and the CH stretching mode (ν(CH)), respectively, of a methylidyne species (CH). The great similarity in relative mode intensity between the present results and the results of previous studies further supports the assignments of these losses. Compiled in Table 1 are HREELS vibrational frequencies and mode assignments for methylidyne on various transition metals[17,18,20,24,26,28,43,44] and those obtained from $Co_3(\mu_3\text{-CH})(CO)_9$[41] and $Ru_3H_3(\mu_3\text{-CH})(CO)_9$[42] organometallic compounds. The carbon–metal stretch was not clearly observed in all of the above HREELS studies including the present one (see for example spectrum d of Figure 2). Presumably, this feature is convoluted with the δ(CH) mode of methylidyne. Infrared and Raman spectroscopic studies of $Co_3(\mu_3\text{-CH})(CO)_9$[41] and $Ru_3H_3(\mu_3\text{-CH})(CO)_9$[42] compounds indeed show that the carbon–metal stretching mode is weaker in intensity and its frequency close to the frequency of the δ(CH) mode.

Table 1. HREELS Vibrational Frequencies (in cm^{-1} units) and Mode Assignments for Methylidyne on Various Transition Metals and Those Obtained from $Co_3(\mu_3\text{-CH})(CO)_9$ and $Ru_3H_3(\mu_3\text{-CH})(CO)_9$ Organometallic Compounds

mode assignment	Ru(0001)[a]	Ru(11$\bar{2}$0)[a]	Ru(0001)[17-18,20]	Rh(111)[43]	Pd(111)[44]
ν(CH)	3000	3010	3010–3030	3025	3002
δ(CH)	790	830	800	770	762

Pt(111)[24]	Ni(111)[26]	$Co_3(\mu_3\text{-CH})(CO)_9$[41]	$Ru_3(\mu_3\text{-CH})H_3(CO)_9$[42]
3100	2980	3041	2988
850	790	850	894

[a] The present work.

The assignment of this set of loss features at ~800 and 3000 cm^{-1} to benzene (C_6H_6) is positively excluded because no loss feature was found in the 900–1500-cm^{-1} frequency range in spectra d and e of Figure 2 or in the spectra of Figure 3. The ring stretching and deformation modes ($\nu_9 \simeq 1330$ cm^{-1}, $\nu_{13} \simeq 1420$ cm^{-1}) and

(41) Howard, M. W.; Kettle, S. F.; Oxton, I. A.; Powell, D. B.; Sheppard, N.; Skinner, P. *J. Chem. Soc, Faraday Trans. 2* **1981**, *77*, 397–404.
(42) Oxton, I. A.; *Spectrochim. Acta A* **1982**, *38*, 181–184.
(43) Dubois, L. H.; Somorjai, G. A. *ACS Symp. Ser.* **1980**, *32*, 1.
(44) Gates, J. A.; Kesmodel, L. L. *Surf. Sci.* **1983**, *124*, 68–86.

the CH bending mode ($\nu_{10} \simeq 1120$ cm^{-1}) of benzene have been observed in this frequency range.[45,46] The work of Ceyer et al. has also shown that the benzene synthesized from methyl species desorbs or decomposes on Ni(111) at temperatures below ~400K.[47]

Information relevant to the adsorption site of CH on the Ru(0001) and Ru(11$\bar{2}$0) surfaces may be deduced from the observed vibrational losses. The frequency of the δ(CH) mode is consistently higher on Ru(11$\bar{2}$0) than on Ru(0001). The difference in frequency of 40 cm^{-1} exceeds the experimental error bars (about $\pm$10 cm^{-1} in the present case). Considering the surface geometry of the two surfaces, adsorption of CH onto threefold hollow sites is most likely. As shown in Figure 1, the threefold site on Ru(11$\bar{2}$0) involves a Ru atom of the second layer and thus differs from the threefold site on Ru(0001). The bonding of a methylidyne species to either the terminal or bridge site is expected to give rise to the same frequency of the δ(CH) mode, since these sites have a similar environment on both surfaces. Previous theoretical studies also have indicated that a CH intermediate is preferentially adsorbed onto a threefold site.[11]

Figure 4 shows that the change of the δ(CH) mode as a function of the off-specular angle parallels in intensity the change of the elastic peak. This feature indicates the dipole nature of the δ(CH) mode, whereas the ν(CH) mode of methylidyne is predominantly excited by impact scattering. In order for the bending mode to be dipole active on the Ru(0001) surface, the CH bond must be skewed to the surface normal due to the surface selection rule.[48] Such bonding geometries with the CH bond inclined to the surface have first been proposed for a CH species on Ni(111) by Demuth and Ibach.[28]

Our studies on the thermal stability of the ~800- and ~3000-cm^{-1} losses further support the assignment of these losses to a methylidyne species. Figures 3, 6, and 7 show that the methylidyne species decomposes on the Ru surfaces at ~600 K, and the loss features of this species disappear completely at temperatures exceeding 700 K. A CH species from the decomposition of acetylene or ethylene has been previously found to be stable up to ~500 K on several transition-metal surfaces.[17,18,26,29] Weinberg and co-workers,[17,18] for example, have reported that a methylidyne adsorbate obtained from ethylene/acetylene on Ru(0001) decomposes with hydrogen evolution between approximately 500 and 700 K. On Ni(111)[26] and Fe(110)[29] surfaces, a CH species was found to be stable up to at least 500 K. With consideration of the above comparisons and discussion, we conclude that methylidyne intermediates are present on both the Ru(0001) and Ru(11$\bar{2}$0) surfaces following methane decomposition. The likely bonding picture for CH on the Ru surfaces involves interactions between a threefold site of the surface and the carbon atom of the methylidyne species with the CH bond inclined with respect to the surface normal.

The presence of a methyl species (CH_3) after methane activation on the Ru surfaces under the reaction conditions employed here was neither observed nor expected. The work of Ceyer and co-workers[27] has clearly demonstrated that methyl intermediates on Ni(111) decompose well below room temperature (at ~200 K) to produce a CH species. The presence of methylidene intermediates can also be excluded on the basis of the observed vibrational losses. The following section deals with this issue in further detail.

4.1.2. C_2 Species: Vinylidene. In addition to the losses associated with the methylidyne species, there is the second set of losses observed on both surfaces. On Ru(11$\bar{2}$0), the appearance of the loss feature at 1620 cm^{-1} is a clear indication of a carbon–carbon double bond because this loss energy exceeds the frequencies of vibrational modes involving hydrogen. The losses at ~345, 1165, 1410, 1620, and 2985 cm^{-1} (see Figures 5–7) are then attributed to the carbon–metal stretch ($\nu(CCH_2$–Ru), the CH_2 rock ($\rho(CH_2)$), the CH_2 scissors ($\delta(CH_2)$), the carbon–carbon stretch (ν(C=C)), and the CH_2 stretch ($\nu(CH_2)$), respectively, of a vinylidene intermediate (CCH_2). The assignment to a vinyl species ($CH{=}CH_2$) is excluded for the following reason: (1) The CH unit of a vinyl species should give rise to three additional peaks associated with CH bending and stretching in the vibrational spectra. Infrared and Raman spectra of $HOs(CH{=}CH_2)(CO)_{10}$,[49] for example, have shown that bands at 782, 1266, and 2920 cm^{-1} are due to the excitations of the out-of-plane CH bending, in-plane CH bending, and CH stretching, respectively, of the CH unit of vinyl ligands. These modes are not observed in our HREELS spectra. (2) The bonding of a vinyl species to the surface is expected to be weaker than that of vinylidene. The observation of the vinylidene at high temperatures (as shown in Figures 5–7) suggests that the CCH_2 species in the present case is stable. This stability is consistent with the above considerations.

Hills et al.[50] have isolated a vinylidene species from the dehydrogenation of ethylidyne on an oxygen predosed Ru(0001) surface. By analogy to the bonding of the vinylidene ligand in $H_2Os_3(CCH_2)(CO)_9$,[49] these authors proposed that the vinylidene species is bonded to the surface via nearly sp^2-hybridized carbon atoms with its carbon–carbon bond skewed about the surface plane. In this adsorption geometry, a downward shift in the ν(C=C) frequency of the adsorbed vinylidene to 1435 cm^{-1} (compared to an unperturbed carbon–carbon double bond of ~1600 cm^{-1})[51] was observed. The weakening of the carbon–carbon double bond is due to π-electron donation from the double bond to the surface. Therefore, the high frequency of the ν(C=C) mode observed in the present case indicates a largely unperturbed carbon–carbon double bond of CCH_2 on Ru(11$\bar{2}$0). We therefore conclude that vinylidene is bonded to Ru(11$\bar{2}$0) via only a single carbon atom.

In contrast to the case of decomposition of methane on Ru(11$\bar{2}$0), the second set of losses contains only two weak loss peaks on Ru(0001). The observation of the 1395-cm^{-1} loss, which corresponds to the scissors mode of CH_2, indicates the existence of CH_2 groups on Ru(0001). The possibility for CH_3 groups is rejected, since the symmetric (at ~1350 cm^{-1}) and asymmetric (at ~1425 cm^{-1}) deformation of CH_3 was not observed. Furthermore, the corresponding spectrum acquired at an off-specular direction (not shown here) revealed only one peak at ~1400 cm^{-1} that is attributed to the scissor mode of CH_2 groups.

However, we identify the species corresponding to the above losses as a vinylidene species rather than as a methylidene species for the following reasons: (1) The methylidene species (CH_2) isolated from the decomposition of both ethylene and diazomethane on Ru(0001) has been characterized using HREELS by George et al.[52] The spectrum of the methylidene on Ru(0001) exhibited loss features different from those obtained in the present study. The intense peak at 900 cm^{-1}, attributed to a CH_2 twist, for example, is absent in spectra b and c of Figure 2. (2) In the 500–550 K temperature range, in which the two features at 1160 and 1395 cm^{-1} were observed in the present study, the methylidene species was found either to decompose

(45) Mate, C. M.; Somorjai, G. A.; *Surf. Sci.* **1985**, *160*, 542–560.
(46) Koel, B. E.; Crowell, J. E.; Mate, C. M.; Somorjai, G. A. *J. Phys. Chem.* **1984**, *88*, 1988–1996.
(47) Yang, Q. Y.; Johnson, A. D.; Maynard, K. J.; Ceyer, S. T. *J. Am. Chem. Soc.* **1989**, *111*, 8748–8749.
(48) Ibach, H.; Mills, D. L. *Electron Energy Loss Spectroscopy and Surface Vibrations*, Academic: New York, 1982.
(49) Andrews, J. R.; Kettle, S. F. A.; Powell, D. B.; Sheppard, N. *Inorg. Chem.* **1982**, *21*, 2874–2877.
(50) Hills, M. M.; Parmeter, J. E.; Weinberg, W. H. *J. Am. Chem. Soc.* **1987**, *109*, 597–599.
(51) Maslowsky, E., Jr. *Vibrational Spectra of Organometallic Compounds*; John Wiley & Sons: New York, 1977; p 233.
(52) George, P. M.; Avery, N. R.; Weinberg, W. H.; Tebbe, F. N. *J. Am. Chem. Soc.* **1983**, *105*, 1393–1394.

Table 2. HREELS Vibrational Frequencies (in cm^{-1} units) and Mode Assignments for Vinylidene on Ru(11$\bar{2}$0), Ru(0001), and O/Ru(0001) and Those Obtained from a $Os_3H_2(CCH_2)(CO)_9$ Organometallic Compound

mode assignment	Ru(0001)[a]	Ru(11$\bar{2}$0)[a]	O/Ru(0001)[50]	$Os_3H_2(CCH_2)(CO)_9$[49]
$\nu_a(CH_2)$			3050	3052
$\nu_s(CH_2)$		2985	2985	2990
ν(CC)	1160	1620	1435	1467
$\delta(CH_2)$	1395	1410	1435	1328
$\rho(CH_2)$		1165	965	1048
$\omega(CH_2)$			895	959
$\tau(CH_2)$				808
ν(MC)		345	455	255–311

[a] The present work.

into methylidyne and carbon on Ru(0001)[52] or to convert to a vinylidene species on Fe(110).[53]

Considering the above discussion, we thus attribute the losses at 1165 and 1395 cm^{-1} to the carbon–carbon stretch (ν(C=C)) and the CH_2 scissor mode ($\delta(CH_2)$), respectively, of a vinylidene intermediate. Note that the carbon–carbon double bond of the vinylidene is partially reduced on Ru(0001), as suggested by the low ν(C=C) frequency of 1165 cm^{-1}. This feature implies that both carbon atoms are inclined with respect to the surface and the vinylidene double bond is interacting directly with the surface. Compiled in Table 2 are HREELS vibrational frequencies and mode assignments for vinylidene on Ru(11$\bar{2}$0), Ru(0001), and O/Ru(0001)[50] and those obtained from organometallic compounds.[49]

4.1.3. C_2 Species: Ethylidyne. The third set of losses observed only in the 330–400 K temperature range on Ru(11$\bar{2}$0) has been attributed to a new species in our Results section. The observation of the 1370- and 1440-cm^{-1} losses is a clear indication for the presence of CH_3 groups. These two features correspond to the symmetric and asymmetric deformation of a methyl species. By comparison to the results obtained from HREELS studies[17,18,21–24]and those of organometallic compounds,[54] we identify this new species as an ethylidyne species. Compiled in Table 3 are HREELS vibrational frequencies and mode assignments for ethylidyne on various transition metals[17,18,21–24] and those obtained from the $Co_3(\mu_3\text{-}CH_3C)(CO)_9$ organometallic compound.[54] The assignment to methyl is excluded by considering the thermal stability of the methyl species.[27] The possibility for an ethylidene (CH_3CH) species is also rejected on the basis of the same reasoning used to eliminate a vinyl species (see section 4.1.2 for details).

4.1.4. Graphitic Carbon. One loss feature left unexplained is the one that is barely perceptible between approximately 1100 and 1500 cm^{-1} in Figure 3, and also in Figures 6 and 7c and d. Spectrum d of Figure 3, for example, appears to be nearly indistinguishable from that of the clean surface; however, the difference in TPD spectra following CO adsorption between the surface corresponding to spectrum d of Figure 3 and the clean surface is evident, as shown in Figure 8. The integrated area of the CO TPD from the former is only 30% of that of the clean surface. CO titration was also carried out on the Ru(0001) surface immediately after the reaction without a high-temperature anneal. Displayed in Figure 8a is a CO TPD spectrum acquired after methane decomposition on the Ru(0001) surface at 600 K. The integrated area of the CO TPD is only a few percent of that of the clean surface. This result is not surprising, since the surface in this case is saturated by the methylidyne species, as discussed in section 4.1.1. Upon heating the surface to temperatures >800 K, the CH species decomposes, leaving surface carbon on the surface. At these high temperatures, the surface carbon species likely undergoes agglomeration, forming a surface graphitic phase.

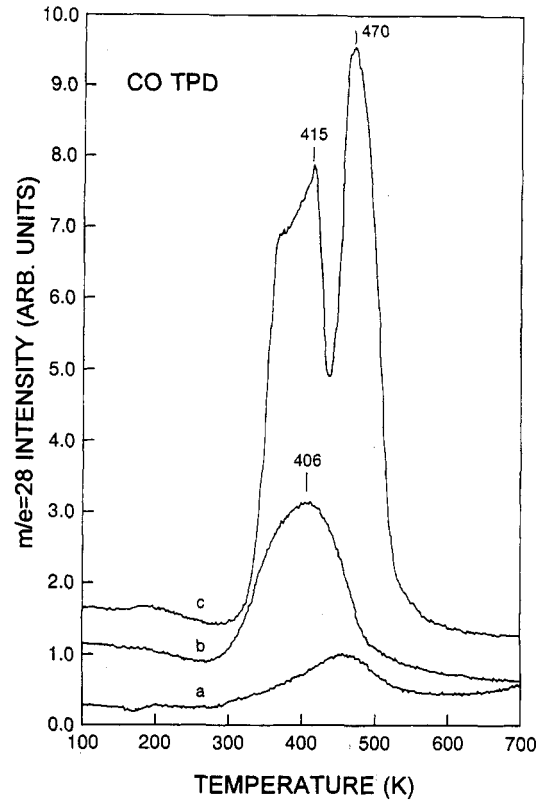

Figure 8. CO TPD spectra obtained following CO saturation exposure: (a) CO TPD spectrum acquired after a Ru(0001) surface is saturated with the methylidyne species; (b) CO TPD obtained from the surface corresponding to the upper spectrum of Figure 3; and (c) CO TPD spectrum of a clean Ru(0001) surface.

This explains why the integrated area of the CO TPD increases from a few percent (Figure 8a) to 30% (Figure 8b) of the CO saturation coverage as the surface is annealed to 800 K. The above explanation is also consistent with our HREELS measurements. The very weak feature observed at 1100–1500 cm^{-1} likely arises from losses associated with the ring-breathing mode of surface graphite.[55]

4.2. Comparison with Results of the Supported Catalysts. Various forms of surface carbonaceous species from methane decomposition on silica-supported Ru, Rh, and Co catalysts have been investigated by van Santen and co-workers[8–10] using temperature-programmed reaction. Three forms of surface carbon species, designated as C_α, C_β, and C_γ species, are distinguishable from their ability to form methane during hydrogenation. The C_α species appears very active and hydrogenates readily into methane at temperatures near 300 K. This species was considered to be a principal precursor to higher hydrocarbons. A less reactive surface species (C_β) can be hydrogenated between 373 and 573 K and partially converted into the C_α species. Finally, the C_γ species is least active and reacts with hydrogen to produce only methane at temperatures exceeding 673 K. These C_α, C_β, and C_γ species were suggested to correspond to carbidic, amorphous, and graphitic carbon, respectively.[8–10]

There is, however, no spectroscopic evidence in the present study for the carbidic carbon (presumably the atomic carbon) formed following methane decomposition under the reaction conditions employed. Such single carbon atoms should give rise to an intense loss peak at ~550 cm^{-1} in the HREELS spectra.[26] Instead, the methylidyne and vinylidene species were found on both the Ru(0001) and Ru(11$\bar{2}$0) surfaces with the CH species being thermally more stable. The third intermediate (ethylidyne),

(53) McBreen, P. H.; Erley, W.; Ibach, H. *Surf. Sci.* **1984**, *148*, 292–310.
(54) Skinner, P.; Howard, M. W.; Oxton, I. A.; Kettle, S. F. A.; Powell, D. B.; Sheppard, N. *J. Chem. Soc., Faraday Trans.* **1981**, *77*, 1203–1215.
(55) Aizawa, T.; Souda, R.; Ishizawa, Y.; Hirano, H.; Yamada, T.; Tanaka, K.; Oshima, C. *Surf. Sci.* **1990**, *237*, 194–202.

Table 3. HREELS Vibrational Frequencies (in cm^{-1} units) and Mode Assignments for Ethylidyne on Various Transition Metals and Those Obtained from a $Co_3(\mu_3\text{-}CH_3)(CO)_9$ Organometallic Compound

mode assignment	Ru(1120)[a]	Ru(0001)[17]	Pt(111)[24]	Pd(111)[23]	Rh(111)[22]	$Co_3(\mu_3\text{-}CH_3C)(CO)_9$[54]
$\nu_a(CH_3)$		3045	2950		2920	2930
$\nu_s(CH_3)$	2975	2945	2890	2900	2880	2888
$\delta_a(CH_3)$	1440	1450	1420	1400	1420	1420
$\delta_s(CH_3)$	1370	1370	1350	1334	1337	1356
ν(CC)	1085	1140	1130	1080	1121	1163
$\rho(CH_3)$		1000	980		972	1004
ν(MC)	355	480	310–600	409	435	220–555

[a] The present work.

observed only at low temperatures (≤400 K) on Ru(11$\bar{2}$0), can be dehydrogenated to a vinylidene species upon heating to above 500 K, as discussed in section 4.1.3 (Figure 6). Therefore, there appears no direct, one-to-one relationship between the hydrocarbonaceous species observed in our study and the C_α and C_β species distinguished from their hydrogenation reactivity in the study of supported catalysts. However, our combined HREELS/elevated-pressure kinetic studies do show that the vinylidene species is likely to be the key intermediate responsible for higher hydrocarbons. The details of these studies including a correlation between the intermediates characterized by HREELS and gas-phase products measured using gas chromatography are described elsewhere.[56]

Close inspection of the results from the supported catalyst reveals that the C_α and C_β species are associated with hydrogen. The average number of hydrogens contained in the surface carbon species following methane decomposition, for example, is near one in the 550–800 K reaction temperature range. This value was determined by measuring the fraction of methane adsorbed and the amount of hydrogen produced using a quadrupole mass spectrometer.[8-10] This result, in fact, agrees well with the present result in which the methylidyne species are found to be dominant at temperatures above 550 K in the HREELS spectra. Moreover, the results from the supported Ru catalyst[8-10] indicated that higher hydrocarbon production is favorable when the surface hydrocarbon fragments are largely dehydrogenated. The optimum average number of hydrogens contained in the surface hydrocarbon fragments was again found to be near one.

In agreement with the results from the supported catalyst,[8-10] a passive form of carbon observed at temperatures exceeding 600 K is present on both the Ru(0001) and Ru(11$\bar{2}$0) surfaces. This unreactive carbon corresponds to the graphitic carbon or the C_γ carbon.

5. Summary

HREELS spectroscopy has been used to characterize various forms of adsorbed hydrocarbon intermediates present on single-crystal Ru catalysts following methane decomposition. Four distinct forms of surface species were identified; these are methylidyne (CH), vinylidene (CCH_2), ethylidyne (CCH_3), and graphitic carbonaceous species. On the Ru(0001) surface, only the methylidyne, vinylidene, and graphitic carbon species were observed. However, the four surface species were all present on the Ru(11$\bar{2}$0) surface.

The methylidyne species was found to be present on both the surfaces in a wide temperature range (between approximately 400 and 700 K). It is characterized by a distinct mode intensity pattern in the HREELS spectra, with a dominant loss feature at ~800 cm^{-1} and a weak feature at ~3000 cm^{-1}. These two losses are due to excitations of the CH bend (δ(CH)) and the CH stretch (ν(CH)), respectively. Off-specular HREELS measurements revealed that the δ(CH) mode is strongly dipole allowed, whereas the ν(CH) mode of methylidyne is predominantly excited by impact scattering.

The vinylidene species was found to be less thermally stable than the methylidyne species on both the Ru surfaces. On Ru(0001), this intermediate was observed at temperatures between 500 and 550 K and was found to bond to the surface with both carbon atoms inclined with respect to the surface. In contrast, the vinylidene species bonds to the Ru(11$\bar{2}$0) surface via only a single carbon atom. This intermediate was observed in the 500–600 K temperature range on Ru(11$\bar{2}$0).

The third species, ethylidyne, exists only on the Ru(11$\bar{2}$0) surface below 400 K and dehydrogenates to vinylidene upon heating. This species is characterized by the symmetric and asymmetric deformation modes of the CH_3 groups.

An unreactive, graphitic-like carbon species was found at temperatures exceeding 600 K and is associated with a very weak feature found between 1100 and 1500 cm^{-1} in the specular HREELS spectra. This graphitic-like carbon can be detected by CO titration.

Acknowledgment. We acknowledge the support of this work by the Gas Research Institute and the Alternative Feedstock Division of Amoco Corporation.

(56) Wu, M.-C.; Lenz-Solumun, P.; Goodman, D. W. *J. Vac. Sci. Technol.* Submitted for publication.